FACTA UNIVERSITATIS
Series: **Working and Living Environmental Protection** Vol. 21, Nº 2, 2024, pp. 119 - 131
https://doi.org/10.22190/FUWLEP240904011D

Original Scientific Paper

THE INFLUENCE OF SAFETY DIODES ON THE CHARACTERISTICS OF THE PHOTOVOLTAIC PANELS UNDER NON-UNIFORM ENVIRONMENTAL CONDITIONS

UDC 621.382:541.13

Marko A. Dimitrijević, Milutin P. Petronijević

Faculty of Electronic Engineering, University of Niš, Serbia

ORCID iDs: Marko A. Dimitrijević https://orcid.org/0000-0001-9032-9595
Milutin P. Petronijević https://orcid.org/0000-0003-2396-0891

Abstract. *The operation of photovoltaic systems depends on the environmental conditions, which affect the current-voltage characteristics of photovoltaic modules and more complex structures. Under non-uniform environmental conditions - different illumination of cells within one module - the characteristics of the module can be increasingly complex. Safety bypass diodes, which are connected in parallel with the cells and protect them from overheating during partial shading, also contribute to this complexity. In order to evaluate the performance of the photovoltaic system, specifically the inverter and the algorithm for maximum power point tracking, it is necessary to take into account these influences on the characteristics of the photovoltaic structures. In this manuscript, the influence of illumination and temperature on individual photovoltaic cells, the topology of a photovoltaic module including bypass diodes, as well as the characteristics of modules with protective bypass diodes under non-uniform environmental conditions are discussed.*

Key words: *photovoltaic cell, photovoltaic module, bypass diodes, current-voltage characteristics*

1. INTRODUCTION

The climate has undergone significant changes in the past hundred years [1], mostly caused by anthropogenic factors. Some of the most significant changes are global warming, ocean acidification, and changes in ecosystems. The Earth's average surface temperature has increased by approximately 1.2°C since the end of the 19th century. Most of the warming has occurred in the past four decades. The oceans have absorbed much of this increased heat, with a temperature rise of more than 0.2°C in half of a century. The direct consequences of global warming are shrinking ice sheets, glacial

Received September 4, 2024 / Accepted October 11, 2024
Corresponding author: Marko A. Dimitrijević
Faculty of Electronic Engineering, Aleksandra Medvedeva 4, 18000 Niš, Serbia
E-mail: marko@venus.elfak.ni.ac.rs

retreat and decreased snow cover. The acidity of surface ocean waters has increased by about 26% since the beginning of the Industrial Revolution [2, 3]. Global sea level has risen about 21cm since the beginning of the 20th century. The rate in the last two decades, however, is nearly double that of the last century and is accelerating slightly every year [4].

Climate change has a direct impact on changes in wildlife and ecosystems [5]. Many species are shifting their geographic ranges, seasonal activities, migration patterns, and interactions with other species in response to climate change. Indirectly or directly, it also affects human lives. We are witnessing an increase in the frequency and intensity of extreme weather events, including heatwaves, heavy rainfall, droughts, and hurricanes [6]. Denying climate change is increasingly meaningless.

These changes are largely attributed to increased concentrations of greenhouse gases, such as carbon dioxide (CO_2), methane (CH_4), and nitrous oxide (N_2O), resulting from human activities: mostly burning fossil fuels, deforestation, and industrial development.

With the growing awareness of global climate change, efforts to reduce it have also intensified. As these changes are mainly caused by the ever-increasing need for energy production and the consequently enormous use of fossil fuels, most efforts have been made to find new, cleaner energy sources. In response to these challenges, the global and mass usage of photovoltaic technologies began at the beginning of the century. In 2023 alone, the total capacity of solar power plants installed around the planet has increased by 410GW, which is almost half of the previously installed capacity [7].

A large share of the total photovoltaic capacity comprises residential systems connected to the power grid [8]. One such system consists of a photovoltaic (PV) array, DC to AC converter – PV inverter, and optional energy storage – battery. The PV inverter is equipped with a controller whose function is to determine the maximum power operating point of the PV array. The controller achieves this by executing the Maximum Power Point Tracking (MPPT) algorithm. There are several implementations of the MPPT algorithm, a detailed description of their implementations and characteristics is described in [9-11].

The basic photovoltaic component is the photovoltaic cell [12]. The voltage generated by the cell is between 0.5V and 0.6V. To achieve the appropriate voltage for conversion, multiple cells are connected in a photovoltaic module (panel) with a series connection, and the modules are connected in series in a photovoltaic string [13]. Finally, multiple strings are connected in parallel or in series in a structure called a photovoltaic array to generate the necessary DC power.

The current-voltage (I-V) characteristic of the PV array will depend on the characteristics of the individual cells, as well as the way they are connected into modules, i.e. strings and arrays. If the array is formed from modules with the same characteristics, and if all modules work under the same, uniform environmental conditions (illumination, temperature), the shape of the I-V characteristic of the array will have the same shape as the characteristic of the individual cell. However, in real (non-uniform) environmental conditions, the I-V characteristics of the cells will be different, and the resulting characteristic of the entire array will be more complex. Moreover, PV modules contain safety diodes that affect the equivalent characteristics.

Operation of the PV inverter, i.e. conversion of DC to AC voltage, more precisely the maximum achievable power depends on the characteristic of the array to which it is connected. Knowing the shape of the PV array characteristic, as well as its dependence on array topology and environmental conditions, is therefore important.

This paper will summarize the operation mode of the PV cell and PV module, with special reference to the operation in non-uniform conditions. The function of safety diodes will be explained, as well as their influence on the characteristics of PV modules. The characteristics of more complex PV structures can be derived based on the characteristics of the modules and how they are connected.

The manuscript is organized as follows: Section 2 presents the operation of the photovoltaic cell, its most used single-diode model, and the equation that describes the current-voltage characteristic of the cell based on the given model. Also, the dependence of the characteristics on environmental conditions, specifically illumination and temperature, was elaborated. Section 3 describes the PV module, and its operation under uniform environmental conditions and under partial shading, i.e. different cell illumination. Finally, the function of safety diodes is presented and their influence on the I-V characteristic of the module is discussed in detail. Section 4 concludes the manuscript.

2. THE CHARACTERISTICS OF PV CELL

A photovoltaic (PV) cell is a semiconductor device that converts visible or near-visible electromagnetic radiation into electricity through the photovoltaic effect. Photovoltaic power plants are complex structures that are essentially formed by connecting a large number of photovoltaic cells. The characteristics of these structures depend on the characteristics of the individual cells from which they are made, as well as on the topology, i.e. how the cells are interconnected.

The PV cell is implemented as a semiconductor p-n junction. The p-n junction represents the basic semiconductor structure, which is made by doping the semiconductor with different types of dopants. One part of the junction is a p-type semiconductor, made by doping with acceptors, dopants of the third group of elements of the periodic table, such as boron. The second part of the junction is an n-type semiconductor, made by doping with donors, elements of the fifth group of elements, such as phosphorus.

2.1. The Single-diode model of PV cell

There are several PV cell models, highlighting different cell properties. Most models are static, and are used to model cells in DC operation. In [14, 15] the dynamic characteristics of the PV cell are presented. The simplest static cell model is the single-diode model, which is the most widely used because of its simplicity [16]. In further consideration, for the analysis of static current-voltage (I-V) and power-voltage (P-V) characteristics, this model will be used (Fig 1).

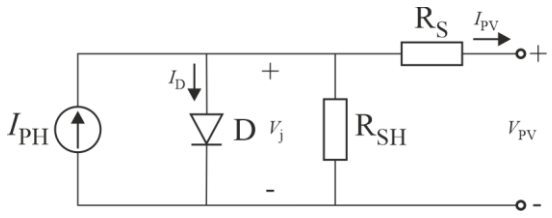

Fig. 1 Singe-diode model of PV cell. R_S is the series resistance, R_{SH} is the parallel

(shunt) resistance of the model.

The dependence of cell current I_{PV} on cell voltage V_{PV} defines the current-voltage characteristic of a PV cell. This dependence, based on the single-diode model shown in Fig. 1, can be represented by the equation:

$$I_{PV} = I_{PH} - I_S\left(e^{\frac{q_e(V_{PV}+I_{PV}R_S)}{nkT}} - 1\right) - \frac{V_{PV}+I_{PV}R_S}{R_{SH}}, \tag{1}$$

where I_{PH} represents photocurrent, I_S is the reverse saturation current of a p-n junction, $q_e$stands for the electron charge (1.6×10^{-19}C), k is the Boltzmann constant (1.38×10^{-23} J/K), T is cell absolute temperature (K), and n is the diode ideality factor.

The single-diode model can be further simplified if the series ($R_S = 0$) and parallel ($R_{SH} = \infty$) resistances of the model are neglected.

The equation **Error! Reference source not found.** is a non-linear equation, and the current I_{PV} figures are on both sides of the equation. Furthermore, I_{PV} exists in both the linear term and the exponent on the left-hand side of the equation. However, by applying the Lambert W-function [17], it is possible to obtain an explicit current-voltage dependence of the PV cell [18]:

$$I_{PV} = \frac{I_{PH}+I_S-V_{PV}/R_{SH}}{1+R_S/R_{SH}} - \frac{nV_T}{R_S}W\left(\frac{I_S R_S}{nV_T\left(1+R_S/R_{SH}\right)}e^{\frac{V_{PV}}{nV_T}\left(1-\frac{R_S}{R_S+R_{SH}}\right)+\frac{(I_{PH}+I_S)R_S}{nV_T(1+R_S/R_{SH})}}\right), \tag{2}$$

where $V_T = \dfrac{kT}{q_e}$ represents thermal voltage.

2.2. The current-voltage characteristics

The current-voltage (I-V) characteristic of the PV cell, for $I_{PH} = 8.24$A, $I_S = 2.36$nA, $R_{SH} = 1000\Omega$, $R_S = 0.002\Omega$, $n = 1.3$ and at temperature $T = 298$K is shown in Fig. 2. The characteristic is obtained by means of simulation, using *pvlib* library for Python [19].

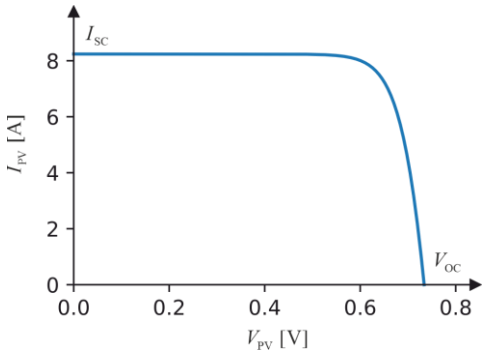

Fig. 2 The current-voltage characteristic of PV cell. I_{SC} represents the short-circuit current and V_{OC} is the open-circuit voltage of the PV cell.

Two terminal points can be observed on the characteristic, the first is a short-circuit of the PV cell ($I_{PV} = I_{SC}$, $V_{PV} = 0$) and the second is an open-circuit ($I_{PV} = 0$, $V_{PV} = V_{OC}$). If the resistances in the single-diode model are ignored, according to the equation **Error! Reference source not found.**, approximate values for the short-circuit current and open-circuit voltage can be calculated as:

$$I_{SC} \approx I_{PH}, \tag{3}$$

$$V_{OC} \approx \frac{nkT}{q_e} \ln\left(\frac{I_{PH}}{I_S} + 1\right). \tag{4}$$

2.3. The temperature and illumination dependence

The characteristic of the PV cell depends on the environmental conditions, i.e. illumination and temperature. In addition to the explicit temperature dependence, which can be observed in the equation **Error! Reference source not found.**, other parameters also depend on environmental conditions. The reverse saturation current of the p-n junction has a complex dependence on temperature [20]:

$$I_S \sim T^{\frac{3}{n}} e^{\frac{E_g}{nkT}} \tag{5}$$

where E_g is the band-gap of the cell material (1.12eV for silicon).

The dependence of the photocurrent on temperature T and illumination G is approximately linear, therefore an empirical formula is used for its Anderson translation model [21]:

$$I_{PH} = (I_{STC} - \beta(T - T_{ref})) \cdot \frac{G}{G_{ref}} \tag{6}$$

where I_{STC} is short-circuit current under standard testing conditions, defined with $T_{ref} = 298K$ and $G_{ref} = 1000W/m^2$, and β represents the current temperature coefficient (A/K). The illumination and temperature dependencies of the I-V characteristic of the PV cell are shown in Fig. 3.

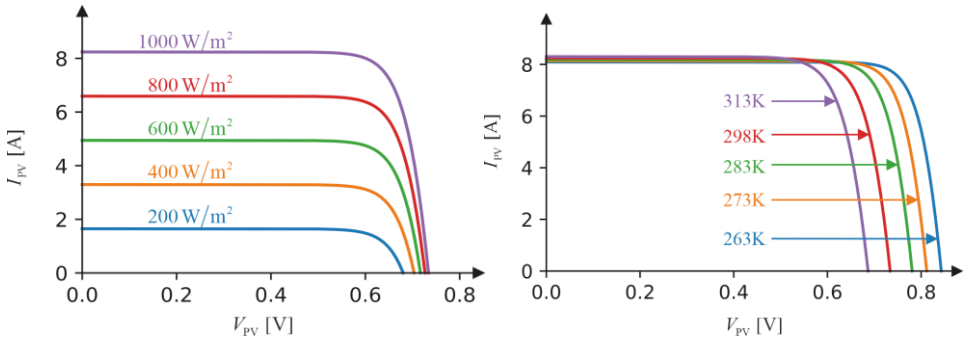

Fig. 3 The PV cell characteristics for different illuminances, from 200 W/m^2 to 1000 W/m^2 at the same temperature, $T_{ref} = 298K$ (left) and for different temperatures, from 263K to 313K at the same illumination, $G_{ref} = 1000W/m^2$ (right).

3. PHOTOVOLTAIC MODULE

3.1. Photovoltaic module under uniform illumination

Photovoltaic (PV) modules are monolithic structures made by a series of connections of cells implemented in the same technology. Therefore, the I-V characteristics of all cells within one module are almost identical under uniform illumination and temperature of the module. In this case, the equivalent module I-V characteristic can be calculated according to the Kirchoff voltage law (KVL). As the cells are connected in series, the current flowing through each cell is the same and it is also the output current of the module. According to KVL, the output voltage of the module is equal to the sum of the cell voltages. The equivalent I-V characteristic of a module resembles the shape of individual cell characteristics, with identical current and voltage multiplied by the number of cells in the module (Fig. 4, left). The power-voltage (P-V) characteristic, the power dependence on the voltage of the module under conditions of uniform illumination has one maximum – maximum power point (Fig. 4, right).

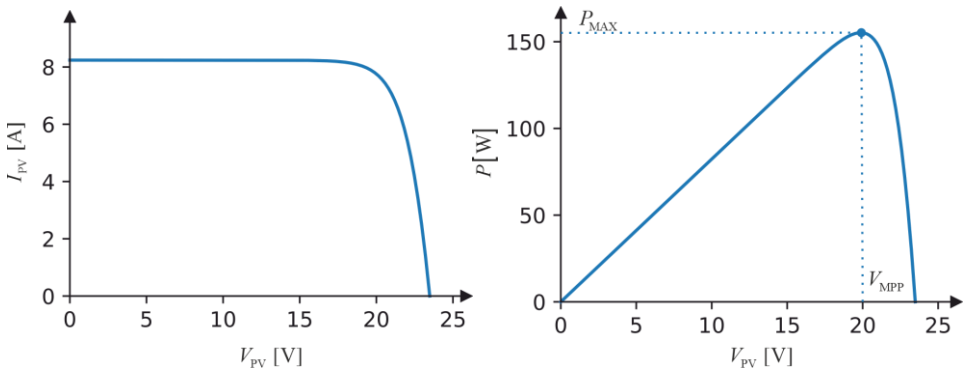

Fig. 4 I-V characteristic of PV module (left) and P-V characteristic (right). Maximal power is achieved for maximum power point voltage V_{MPP}.

3.2. Photovoltaic module under nonuniform illumination

However, in real exploitation, individual cells within the module may be shaded, soiled, or heated differently. Thus, cells under different conditions have different short-circuit current and open-circuit voltage, hence different I-V characteristics in general. In order to analyse the operation of a PV module under such nonuniform environmental conditions, the equivalent circuit of a series connection of differently illuminated cells is used as a simple model, shown in Fig. 5.

For the sake of simplicity, a single-diode model with $R_S = 0$ and $R_{SH} = \infty$ is used. One cell in a series connection is shaded, producing photocurrent I_{PH2}, and other n cells are fully illuminated, generating I_{PH1}. The short-circuit current of the described topology is limited to the smallest photocurrent in serial connection, i.e. to the photocurrent of the most shaded cell. According to KVL, the voltage of a shaded cell is negative:

$$V_{j2} = -nV_{j1} \tag{7}$$

and the p-n junction of this cell is reverse-biased.

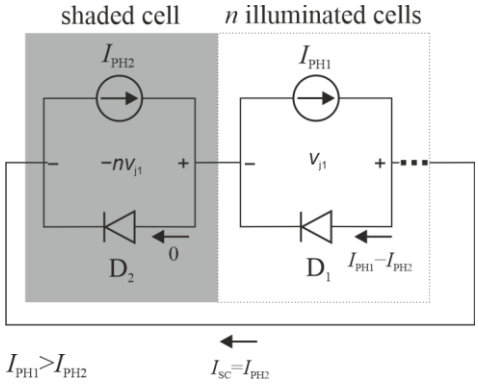

Fig. 5 The series connection of PV cells, one cell is shaded and n cells are fully illuminated. The shaded cell has a smaller photocurrent and limits module current. Furthermore, considerable power is dissipated, leading to the appearance of hot spots and potential damage or destruction.

When a module is short-circuited, considerable power is dissipated on the shaded cell, which can lead to its overheating, the appearance of hot spots on the module, and potential damage.

3.3. The bypass diodes

Dissipation can be reduced by connecting safety diodes - bypass diodes D_{BP} in parallel to the shaded cells, Fig. 6, protecting them from overheating and damage.

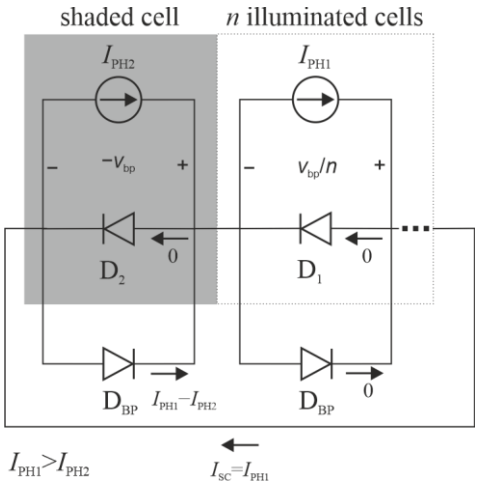

Fig. 6 The bypass diodes connected in parallel to cells.

The bypass diode is connected in opposite polarity to the p-n junction of the cell. When a negative voltage appears due to cell shading, the bypass diode is forward-biased.

The voltage of the shaded cell is equal to forward forward-biased bypass diode p-n junction voltage drop:

$$V_{j2} = -V_{bp}, \tag{8}$$

which is significantly less than in the case without the connected bypass diode. Consequently, the dissipated power on the shaded cell is approximately n times smaller. The bypass diode current is equal to the difference between fully illuminated cell photocurrent and shaded cell photocurrent:

$$I_{bp} = I_{PH1} - I_{PH2}. \tag{9}$$

The short-circuit current of a series connection I_{SC} in this case is equal to a fully illuminated cell photocurrent, I_{PH1}.

The I-V characteristic, determined by the current I_M, of a module containing shaded cells can be calculated using equivalent circuits, shown in Fig. 7 and Fig. 8. If the module is loaded with high resistance, the current of the module, i.e. the series connections of the cells will be less than the photocurrents: $I_{PH1} > I_{PH2} > I_M > 0$. This case is illustrated in Fig. 7.

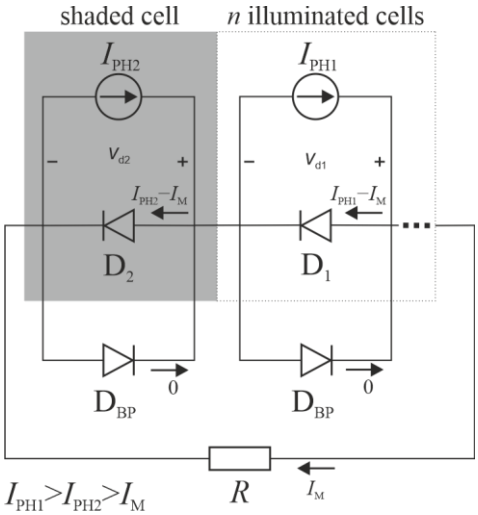

Fig .7 The PV module loaded with high resistance, corresponding to $I_{PH1} > I_{PH2} > I_M > 0$.

The p-n junctions of all the cells within the module are forward-biased and the bypass diodes are reverse-biased so that the total voltage of the module is equal to the sum of the voltages of the individual cells:

$$V_M = V_{j2} + nV_{j1} \tag{10}$$

For $I_{PH1} > I_{PH2} > I_M$, equivalent characteristics can be modelled by summing the cell voltages for the equal cell currents.

The circuit depicted in Fig. 8 corresponds to a low load resistance when the module current is greater than the shaded cell photocurrent, $I_{PH1} > I_M > I_{PH2}$.

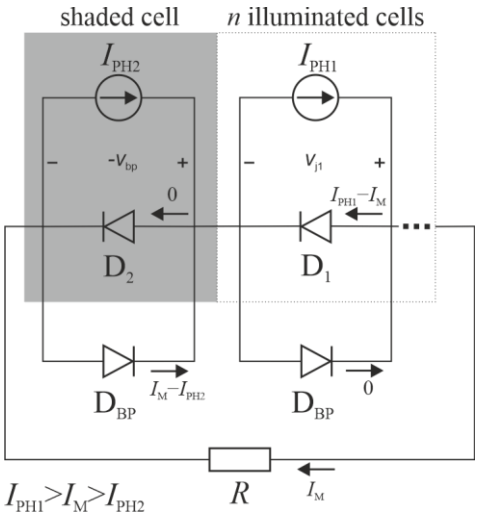

Fig. 8 The PV module loaded with low resistance, corresponding to $I_{PH1} > I_M > I_{PH2}$.

In this configuration, only the p-n junctions of the illuminated cells are forward-biased. The p-n junction of the shaded cell is reverse-biased, and the diode bypassing this cell is forward-biased. The voltage of the module is:

$$V_M = -V_{bp} + nV_{j1}. \tag{11}$$

For $I_{PH1} > I_M > I_{PH2}$, the equivalent characteristic of a module can be modelled by summing only voltages of the fully illuminating cells for the equal currents, and subtracting voltage drop on forward biased bypass diodes.

The previous consideration can be generalized to cases where there are multiple equally shaded cells, or when the illumination of the cells in the module is different.

3.2. Practical implementations of PV modules

In commercial modules, for practical reasons, one bypass diode is connected in parallel with multiple cells. An example of this topology is illustrated in Fig. 9. The module consists of 12 cells connected in series, in such a manner that groups of four cells are protected by one bypass diode. One cell is shaded, and it generates a photocurrent I_{PH2}. Other cells are fully illuminated, generating I_{PH1}. The case where $I_{PH1} > I_M > I_{PH2}$ is illustrated. The p-n junction of the shaded cell is reverse-biased, and the cell voltage is

$$V_{j2} = -V_{bp} - 3V_{j1} \tag{12}$$

which is a four times higher voltage than in the case when each cell is protected by a bypass diode, but still three times less than in the case when the bypass diodes are not connected. When designing a PV module, it is necessary to take into account the maximum power that can be dissipated on the cell, so that damage does not occur. Based on the maximum dissipation and photocurrent at maximum illumination, the optimal number of cells that can be protected by one bypass diode can be determined.

For the given example, the module output voltage is:

$$V_{\mathrm{M}} = -V_{\mathrm{bp}} + 8V_{\mathrm{j1}}. \tag{13}$$

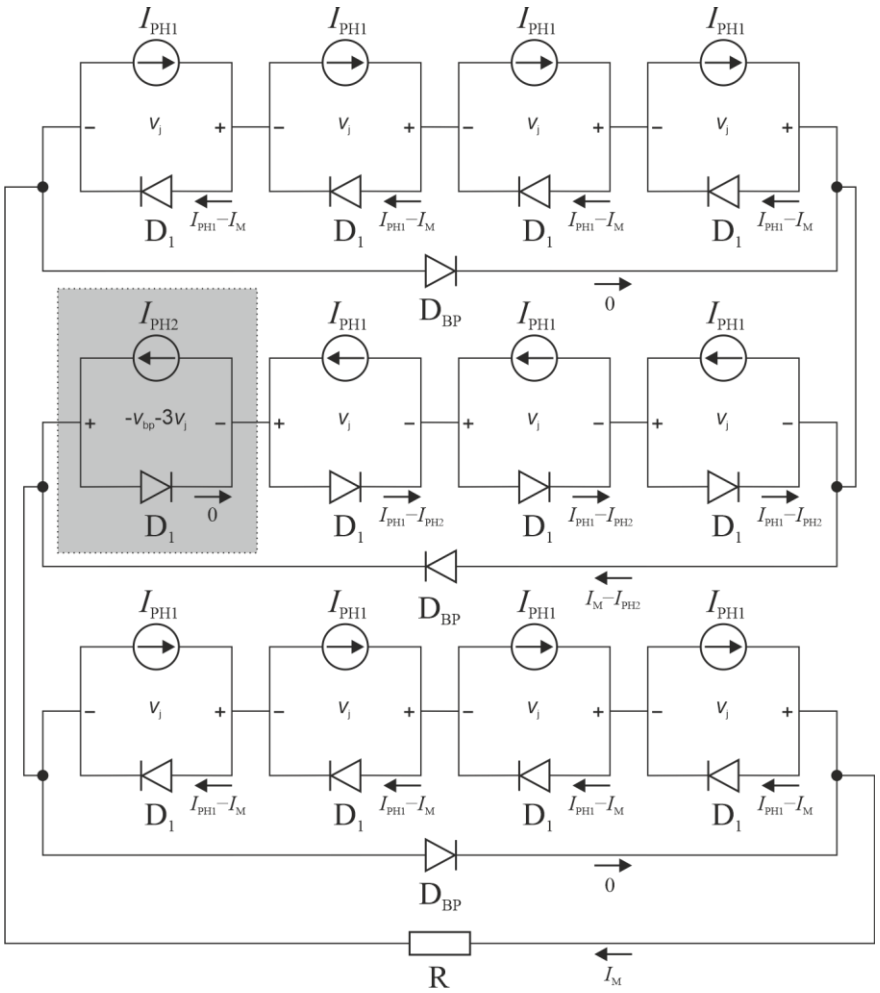

Fig. 9 The PV module with 12 cells, protected with 3 bypass diodes.

3.4. The I-V and P-V characteristics of partially shaded PV module

Based on the previous analysis, it is possible to calculate the I-V and P-V characteristics of a partially shaded PV module based on the known characteristics of individual PV cells for a given illumination.

The example of I-V and P-V characteristics of a PV module under partial shading is shown in Fig. 10. The characteristics shown corresponds to a PV module with 30 cells, of which 24 are fully illuminated, $G = 1000\mathrm{W/m^2}$, while 6 cells are shaded, with $G = 600\mathrm{W/m^2}$. The temperature of all cells is $T_{\mathrm{ref}} = 298\mathrm{K}$.

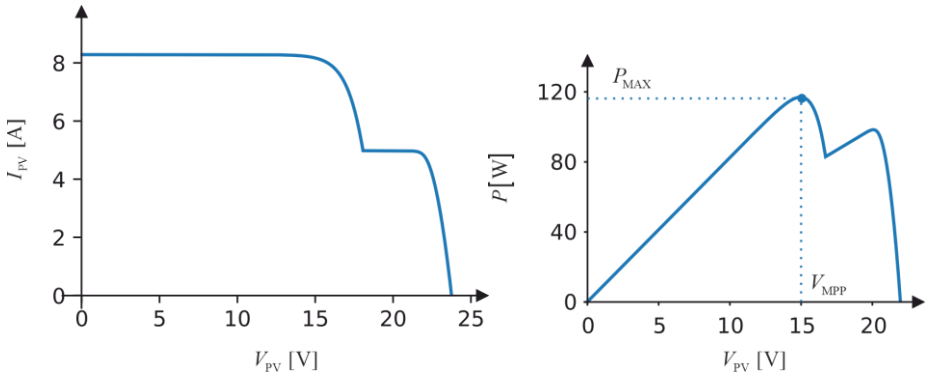

Fig. 10 The simulated I-V and P-V characteristics of the PV module.

The P-V characteristic of partially shaded modules exhibits multiple local maxima, corresponding to different module voltages. The largest of all local maxima is the global maximum – maximum power point P_{MAX}, determined by the voltage V_{MPP}.

4. CONCLUSION

Knowing the I-V and P-V characteristics of the PV module under non-uniform environmental conditions, such as different illumination or temperature of individual cells in the module, is necessary to evaluate the performance of photovoltaic converters operating in real climatic conditions [22]. Those characteristics, as well as characteristics of more complex structures such as strings and arrays, can be increasingly complex depending on the connection of bypass diodes, the topology of the entire PV structure and the shading pattern. The most significant manifestation of this complexity can be observed on the P-V characteristic, in the form of multiple local maxima, which can mislead the MPPT algorithm. For example, many commercial inverters will, in the case of a characteristic similar to the one shown in Fig. 10, select the operating point at the local maximum that is closest to the open-circuit voltage.

There are several tools available to simulate PV modules under different environmental conditions. One of the most used tools is *pvlib*, a library providing a set of classes and methods for simulating PV systems [19]. *Pvlib* can simulate PV cells and modules under conditions of different illumination, which is demonstrated in this manuscript, but cannot generate I-V nor P-V characteristics of modules and series connection of modules that are partially shaded or soiled, nor can take into account the effects of safety bypass diodes in the calculation.

In order to eliminate these shortcomings, a set of classes was developed, which allow the generation of equivalent module characteristics. A detailed description of this software is given in [23]. Using this tool to simulate modules under non-uniform conditions, the characteristics shown in Fig. 10 were generated. This tool enables the generation of characteristics of more complex photovoltaic structures. Both simulated module characteristics, which are presented in this manuscript, and measured module characteristics can be used as input [22].

Acknowledgement: *This manuscript is a part of the research supported by Agreements 451-03-47/2023-01/200102 on the realization and financing of scientific research work of the Faculty of Electronic Engineering, University of Niš in 2024 by the Ministry of Science, Technological Development and Innovation of the Republic of Serbia.*

REFERENCES

1. Lindsey, R. and Dahlman, L. (2021) Climate Change: Global Temperature, https://www.climate.gov /news-features/understanding-climate/climate-change-global-temperature, (accessed 27.7.2024.)
2. Ocean & Climate Platform, (2024) Ocean acidification, https://ocean-climate.org/en/awareness/the-impact-of-climate-change-on-the-ocean/, (accessed 27.7.2024.)
3. Pelejero, Carles; Calvo, Eva; McCulloch, Malcolm T.; Marshall, John F.; Gagan, Michael K.; Lough, Janice M.; Opdyke, Bradley N. (2005). "Preindustrial to Modern Interdecadal Variability in Coral Reef pH". Science. 309 (5744), pp. 2204–2207, doi:10.1126/science.1113692.
4. European Environment Agency, Global and European sea level rise, https://www.eea.europa.eu/ en/analysis/indicators/global-and-european-sea-level-rise (accessed 27.7.2024.)
5. Sattar Q, Maqbool ME, Ehsan R, Akhtar S (2021) Review on climate change and its effect on wildlife and ecosystem. Open J Environ Biol 6(1): 008-014. DOI: 10.17352/ojeb.000021
6. Attribution of Extreme Weather Events in the Context of Climate Change (Report). Washington, DC: The National Academies Press. 2016. pp. 21–24. doi:10.17226/21852. ISBN 978-0-309-38094-2.
7. International Energy Agency, Renewables 2023, Analysis and forecast to 2028, https://iea.blob.core.windows.net/assets/96d66a8b-d502-476b-ba94-54ffda84cf72/Renewables_2023.pdf
8. Residential Solar PV Systems Market, Global Outlook and Forecast 2023-2030, https://www.linkedin.com/pulse/residential-solar-pv-systems-market-global-outlook-oomrf
9. Eltawil, M. A., & Zhao, Z. (2013). MPPT techniques for photovoltaic applications. *Renewable and sustainable energy reviews*, *25*, 793-813.
10. Kamarzaman, N. A., & Tan, C. W. (2014). A comprehensive review of maximum power point tracking algorithms for photovoltaic systems. *Renewable and Sustainable Energy Reviews*, *37*, 585-598.
11. Verma, D., Nema, S., Shandilya, A. M., & Dash, S. K. (2016). Maximum power point tracking (MPPT) techniques: Recapitulation in solar photovoltaic systems. *Renewable and Sustainable Energy Reviews*, *54*, 1018-1034.
12. *Al-Ezzi, Athil S.; Ansari, Mohamed Nainar M. (8 July 2022). "Photovoltaic Solar Cells: A Review". Applied System Innovation. 5 (4): 67. doi:10.3390/asi5040067. ISSN 2571-5577.*
13. *"Photovoltaic... Cell, Module, String, Array". WordPower—Ian Woofenden. 2006. Archived from the original (PDF) on --August 19, 2016. Retrieved December 28, 2018.*
14. Andrejevic-Stosovic, M., Litovski, I., Lukac, D., Dimitrijevic, M., and Litovski, V. (2014). Small signal model of a solar cell. Simulation, Trans. of the Society for Modeling and Simulation, International, pages 1-14.
15. Andrejevic-Stosovic, M., Lukac, D., Litovski, I., and Litovski, V. (2012). Frequency domain characterization of a solar cell. In Proc. of the 11th Symp. on Neural Network Application in Electronic Engineering, NEUREL, pages 259-264.
16. Ćalasan M, Abdel Aleem SHE, Zobaa AF. On the root mean square error (RMSE) calculation for parameter estimation of photovoltaic models: A novel exact analytical solution based on Lambert W function. Energy Convers Manag 2020;210:112716. https://doi.org/10.1016/j.enconman.2020.112716.
17. Wolfram Mathworld, Lambert W-function, https://mathworld.wolfram.com/LambertW-Function.html
18. M. Tripathy, M. Kumar, P.K. Sadhu: Photovoltaic system using Lambert W function-based technique, Solar Energy, Volume 158, 2017, Pages 432-439, ISSN 0038-092X, DOI 10.1016/j.solener.2017.10.007.
19. PV Performance Modeling Collaborative | PV_LIB Toolbox n.d. https://pvpmc.sandia.gov /applications/pv_lib-toolbox/ (accessed March 12, 2023).
20. S. M. Ryvkin, (2014) *Physics of p-n Junctions and Semiconductor Devices*, Springer US.
21. A.J. Anderson, (1996), *Photovoltaic translation equations: A new approach*, Final subcontract report, doi: 10.2172/177401.
22. M. P. Petronijević, I. Radonjić, M. Dimitrijević, L. Pantić, M. Ćalasan, (2024), *Performance evaluation of single-stage photovoltaic inverters under soiling conditions*, Ain Shams Engineering Journal, Volume 15, Issue 1, doi:10.1016/j.asej.2023.102353.
23. M. A. Dimitrijević, M. Petronijević (2024), *Emulation of Photovoltaic Arrays Under Nonuniform Environmental Conditions*, 21st International IGTE Symposium 2024 on Computational Methods in Electromagnetics and Multiphysics, accepted for publication.

UTICAJ SIGURNOSNIH DIODA NA KARAKTERISTIKE FOTONAPONSKIH PANELA U NEUJEDNAČENIM UTICAJIMA SREDINE

Rad fotonaponskih sistema zavisi od uticaja sredine, koji utiču na strujno-naponske karakteristike fotonaponskih modula i složenijih struktura koje se realizuju njihovim povezivanjem. Pri neujednačenim uslovima sredine – različitim osvetljajem ćelija unutar jednog modula – karakteristike modula mogu biti kompleksne. Ovoj kompleksnosti doprinose i sigurnosne bajpas diode, koje su povezano paralelno ćelijama i štite ih od pregrevanja prilikom delimičnog zasenčenja. Kako bi se procenile performanse fotonaponskog sistema, konkretno invertera i algoritma za pronalaženje maksimalne snage, neophodno je uzeti u obzir ove uticaje na karakteristike fotonaponskih struktura. U ovom rukopisu će biti razmotren uticaj osvetljaja i temperature na pojedinačne fotonaponske ćelije, topologija fotonaponskog modula koja uključuje bajpas diode, kao i karakteristike modula sa zaštitnim bajpas diodama pri neujednačenim uticajima sredine.

Ključne reči: *fotonaponska ćelija, fotonaponski modul, bajpas diode, strujno-naponske karakteristike*